

Synthesis and some reactivity of cationic alkyl nitrosyl iridium(III) derivatives

Pietro Diversi ^{a,*}, Fabrizia Fabrizi de Biani ^b, Giovanni Ingrosso ^a, Franco Laschi ^b,
Antonio Lucherini ^a, Calogero Pinzino ^c, Piero Zanello ^b

^a Dipartimento di Chimica e Chimica Industriale dell'Università di Pisa, via Risorgimento 35, I-56126 Pisa, Italy

^b Dipartimento di Chimica, Università di Siena, Pian dei Mantellini 44, I-53100 Siena, Italy

^c Istituto di Chimica Quantistica ed Energetica Molecolare del CNR, via Risorgimento 35, I-56126 Pisa, Italy

Received 4 December 1998; received in revised form 9 February 1999

Abstract

The iridium(III) dimethyl derivatives [Ir(Me)₂Cp*(L)] (Cp* = η⁵-C₅Me₅; L = PPh₃ (**1a**), PMePh₂ (**1b**), PMe₂Ph (**1c**), PMe₃ (**1d**)) react with NOBF₄ in CH₂Cl₂ to give the iridium(III) cationic alkylnitrosyl derivatives [Ir(Me)₂Cp*(NO)]BF₄ (**2**), and [Ir(Me)Cp*(NO)(L)](BF₄)₂ (L = PMePh₂ **4b**, PMe₂Ph **4c**, PMe₃ **4d**). EPR spectroscopy shows that the reaction proceeds through the iridium(IV) intermediates **1a**⁺–**1d**⁺. Treatment of **1d** with NOBF₄ in acetonitrile gives, in addition to **4d**, the acetonitrile substitution products [Ir(Me)Cp*(CH₃CN)(PMe₃)]BF₄ (**5d**) and [IrCp*(CH₃CN)₂(PMe₃)](BF₄)₂ (**6d**). Electrochemical and chemical reduction of **4b**–**4d** afford the corresponding [Ir(Me)Cp*(NO)(L)](BF₄) **7b**–**7d**, which have been studied by EPR spectroscopy. Reaction of **2** with PPh₃ gives [Ir(Me)₂Cp*(PPh₃)]; treatment of **4b** and **4c** with the appropriate phosphine gives [Ir(Me)Cp*(L)₂](BF₄) (L = PMePh₂, PMe₂Ph), respectively. © 1999 Elsevier Science S.A. All rights reserved.

Keywords: Nitrosyls; Iridium; Electrochemistry; EPR

1. Introduction

The iridium(III) dimethyl derivatives [Ir(Me)₂Cp*(L)] (Cp* = η⁵-C₅Me₅; L = PPh₃ (**1a**), PMePh₂ (**1b**), PMe₂Ph (**1c**), PMe₃ (**1d**)) are able to activate aromatic C–H bonds under electron transfer conditions [1]. In the course of an extensive investigation on the redox behaviour of the above systems in the presence of various one-electron oxidants, we have studied the reaction of **1a**–**1d** with NOBF₄ which affords interesting cationic alkylnitrosyl derivatives. In this paper we present the synthesis and characterization of these nitrosyl derivatives of formula [Ir(Me)₂Cp*(NO)]BF₄ (**2**), and [Ir(Me)Cp*(NO)(L)](BF₄)₂ (L = PMePh₂ (**4b**), PMe₂Ph (**4c**), PMe₃ (**4d**)), along with a study of their reactivity towards reduction and displacement reactions. Electrochemical and chemical studies showed that the above dicationic iridium(III) complexes undergo sequential one-electron reductions to the corresponding neutral

congeners. Moreover the above nitrosyl derivatives have been found to undergo an unprecedented NO⁺ substitution reaction by treatment with acetonitrile and phosphines. Part of this study has been published in preliminary form [2].

2. Results and discussion

2.1. Reaction of the iridium(III) dimethyl derivatives [Ir(Me)₂Cp*(L)] (**1a**–**1d**) with NOBF₄ in dichloromethane

The reaction of **1a**–**1d** with NOBF₄ was studied by EPR spectroscopy, carrying out the reaction in the cavity of the spectrometer. The resulting one-electron oxidation products **1a**⁺–**1d**⁺ have been detected at 183 K where single line spectra in solution at *g* = 1.931 (**1a**⁺), 1.939 (**1b**⁺), 1.942 (**1c**⁺) and 1.943 (**1d**⁺) are observed. By lowering the temperature down to 113–123 K, the spectra appear as structured signals, as shown in Fig. 1 for **1b**⁺–**1d**⁺, while raising the temperature causes the signals to disappear gradually.

* Corresponding author. Tel.: +39-50-918225; fax: +39-50-918260.

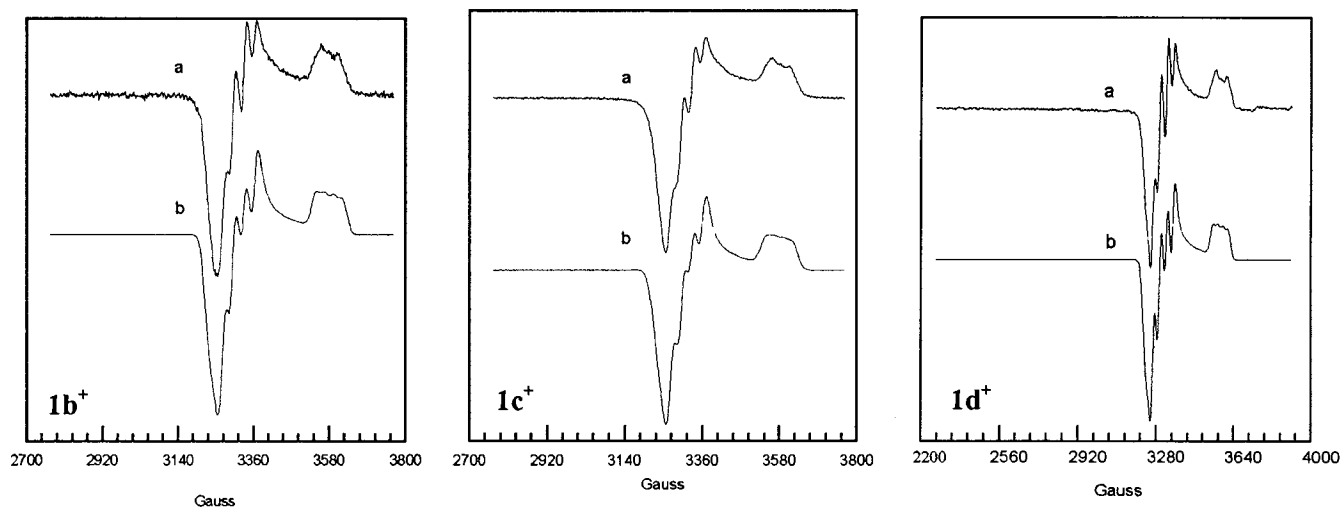


Fig. 1. EPR spectra of the species deriving from the reaction of $\text{Ir}(\text{Me})_2\text{Cp}^*(\text{L})$ ($\text{L} = \text{PPh}_3$ (**1a**), PPh_2Me (**1b**), PPhMe_2 (**1c**), PMe_3 (**1d**)) with NOBF_4 in CH_2Cl_2 . (a) observed spectrum; (b) simulated spectrum.

As already noted [2], the anisotropic spectra implying metal-centred character could be assigned in first approximation to an axial EPR symmetry, where the hyperfine splitting of the perpendicular absorption into a quartet was attributed to spin-coupling to the iridium nucleus (^{191}Ir , 37%; ^{193}Ir , 63%; both $I = 3/2$). However computer simulations by spectral optimization software¹ showed that the spectra of **1a**⁺–**1d**⁺ are better interpreted as corresponding to rhombic EPR symmetry ($g_1 \neq g_2 \neq g_3$; $A_1 \neq A_2 \neq A_3$; all tensor axes coincident), where g_1 and g_2 , because of the linewidths of the resonances, are overlapping (see Fig. 1 and Table 1).

Since the observed hyperfine structure could be due, alternatively, to the interaction of the unpaired electron with the three hydrogen nuclei of an iridium bonded methyl group, we have studied the reaction of $\text{Ir}(\text{Me}-d_3)_2(\eta^5\text{-C}_5\text{Me}_5)(\text{PMe}_3)$ (**1d-d₆**) with NOBF_4 under the same conditions as above. **1d-d₆**⁺ has in solution the same behaviour as the non deuteriated species, showing a large signal centred at $g = 1.942$, which decreases up to disappear on raising the temperature. Moreover the spectrum of **1d-d₆**⁺ in the frozen state at 123 K (Fig. 2) is almost identical to that observed for **1d**⁺ ($g_1 = 2.012$, $g_2 = 1.979$, $g_3 = 1.831$; $A_1 = 19.32$, $A_2 = 30.55$, $A_3 = 24.44$ G): this clearly indicates that the unpaired electron does not interact with the protons of a methyl ligand.

Another possibility was that the spectra could be understood in terms of a rhombic symmetry, the high-field signal resulting from the superimposition of two close components, each appearing as doublet because of the hyperfine interaction with the ^{31}P nucleus ($I = 1/2$) of the phosphine ligand.

¹ The software was provided by the Illinois EPR Research Center, NIH Division of Research, Resonances Grant. No RR01811.

In order to test such possibility, we have reacted the isostructural complex of rhodium(III) $\text{RhMe}_2(\eta^5\text{-C}_5\text{Me}_5)(\text{PMe}_3)$ with NOBF_4 . The EPR spectrum of the resulting oxidation product should present a similar pattern if the above hypothesis was correct. In contrast,

Table 1
X-band EPR parameters of the **1a**⁺–**1d**⁺ species generated by oxidation of **1a**–**1d** with NOBF_4 ^a

Species	g_1	g_2	g_3	$A_1(\text{G})$	$A_2(\text{G})$	$A_3(\text{G})$
1a ⁺	2.067	2.033	1.879	23.46	30.77	26.07
1b ⁺	2.011	1.975	1.830	19.09	30.71	24.01
1c ⁺	2.009	1.977	1.830	20.10	29.60	24.75
1d ⁺	2.013	1.979	1.831	18.08	30.42	22.42

^a Spectra recorded at 113 K in the case of **1a**⁺–**1d**⁺; at 123 K in the case of **1b**⁺–**1c**⁺.

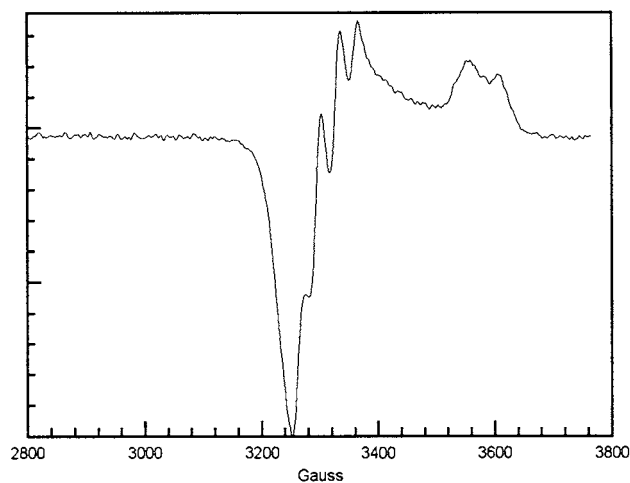


Fig. 2. EPR spectrum of the species deriving from the reaction of $\text{Ir}(\text{CD}_3)_2(\eta^5\text{-C}_5\text{Me}_5)(\text{PMe}_3)$ (**1d-d₆**) with NOBF_4 in CH_2Cl_2 .

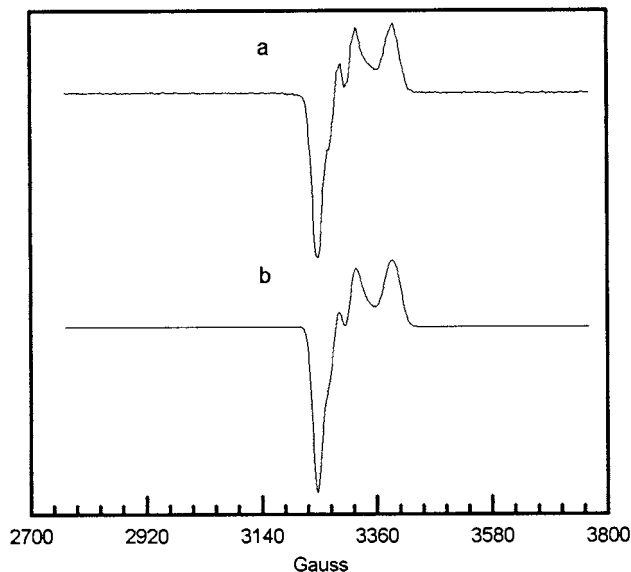


Fig. 3. EPR spectrum of the species deriving from the reaction of $\text{Rh}(\text{Me})_2(\eta^5\text{-C}_5\text{Me}_5)(\text{PMe}_3)$ (**2d**) with NOBF_4 in CH_2Cl_2 . (a) Observed; (b) simulated spectrum.

since rhodium has nuclear spin 1/2, in case of interaction of the unpaired electron with the metal center the spectrum should be simpler and quite different from those observed for the above iridium cations.

This is indeed the case: the spectrum shown in Fig. 3 presents three components, one of these being the sum of two close doublets resulting from the hyperfine coupling of the electronic spin with the rhodium nucleus. The parameters obtained by simulation are the following: $g_1 = 2.018$; $g_2 = 1.989$; $g_3 = 1.932$; $A_1 = 1.37$ G; $A_2 = 30.24$ G; $A_3 = 15.73$ G.

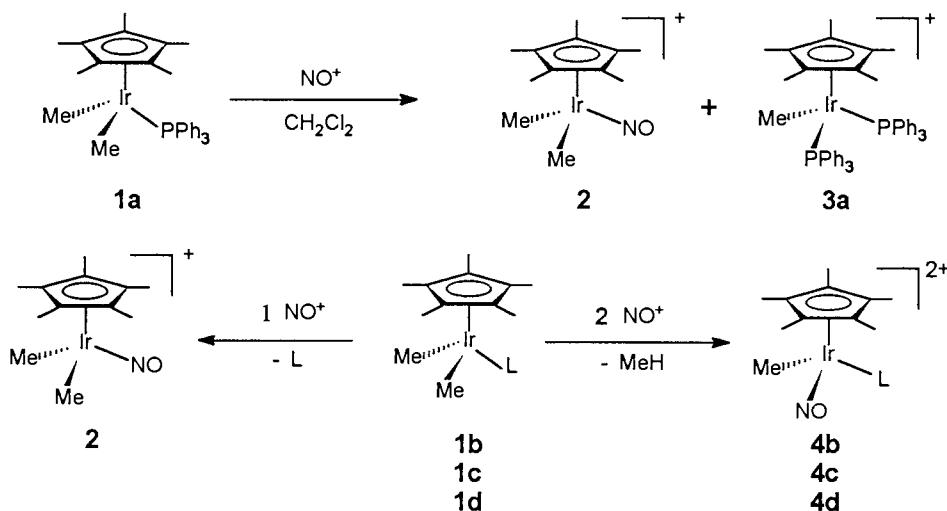
Then the hyperfine coupling constants result from the unpaired electron delocalization on the iridium nucleus, and the species **1a**–**1d**⁺ can be described as low spin cationic complexes of iridium(IV).

On raising the temperature, the intensity of the EPR signals due to **1a**⁺–**1d**⁺ decreases disappearing in the -30 to 0°C range (depending on the nature of the phosphine). By carrying out the reaction at room temperature on a preparative scale, different diamagnetic products are obtained depending on the nature of the phosphine and of the NO^+/Ir ratio.

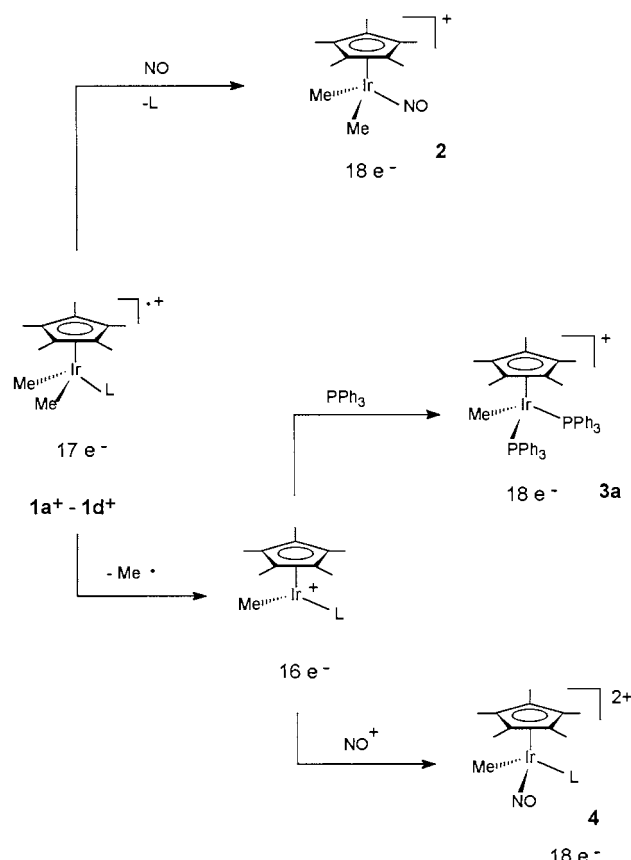
In the case of **1a** by using a NO^+/Ir ratio = 1 a mixture of the cationic nitrosyl derivative $[\text{Ir}(\text{Me})_2\text{Cp}^*(\text{NO})]^+$ (**2**) and of the bisphosphino complex $[\text{Ir}(\text{Me})\text{Cp}^*(\text{PPh}_3)_2]^+$ (**3a**) is formed, and methane is evolved; under the same conditions **1b**, **1c** and **1d** give complicated mixtures which contain **2** as shown by $^1\text{H-NMR}$ spectroscopy. By using a NO^+/Ir ratio = 2, **1a** gives **2** and only small amounts of **3a**; **1b**, **1c** and **1d** afford the dicationic nitrosyl derivatives $[\text{Ir}(\text{Me})\text{Cp}^*(\text{NO})(\text{L})]^2+$ ($\text{L} = \text{PMePh}_2$ (**4b**), PMe_2Ph (**4c**), PMe_3 (**4d**)) (Scheme 1).

The complexes have been characterized by $^1\text{H-NMR}$, IR, MS and carbon and hydrogen elemental analyses. The identity of **3a** was verified by comparison of the $^1\text{H-NMR}$ spectrum with that of an authentic sample prepared by chloride abstraction from $[\text{Ir}(\text{Me})(\text{Cl})\text{Cp}^*(\text{PPh}_3)]$ [3] with AgBF_4 in CH_2Cl_2 in the presence of PPh_3 . All the IR spectra of the above nitrosyl complexes show strong NO absorptions at very high frequencies ($1909 - 1843$ cm^{-1}), pointing to a linear Ir–N–O arrangement.

A common feature of these reactions is the intramolecular formation of methane. In fact by reacting **1a**–**1d** with NO^+ in deuterated solvents, CH_4 forms exclusively (δ 0.20 in CD_2Cl_2 , δ 0.14 in C_6D_6 , δ 0.16 in CD_3NO_2); moreover the $^2\text{H-NMR}$ spectrum of **4d** shows the presence of deuterium on the Cp^* ligand (CD_3NO_2 , δ 2.08). Then the loss of methane occurs intramolecularly and the resulting intermediate (most



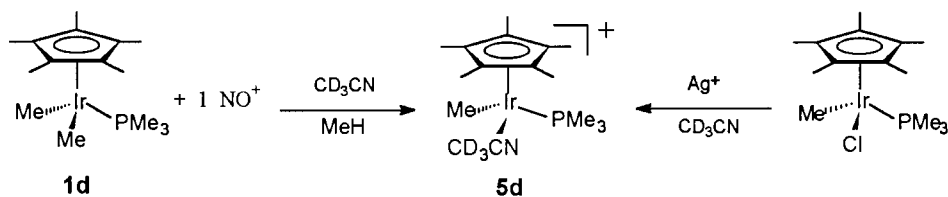
Scheme 1.



Scheme 2.

probably a ‘tucked-in’ species) on its turn abstracts D from the solvent, as it was already observed for related reactions of **1a–1d** [1c,7].

As for the origin of the nitrosyl derivatives, EPR spectroscopic evidences are consistent with the formation of the primary oxidation products $1a^+ - 1d^+$ as the first step. Then, depending on the nature of the phosphine and on the stoichiometry, two reaction patterns are available: the loss of phosphine, followed by coordination of NO, or the loss of methane followed by coordination of phosphine or NO⁺. According to this picture, the **1** → **2** reaction should involve the phosphine displacement by NO in the transient oxidation product **1**⁺, rather than the more common phosphine substitution by NO⁺ from an **1**/NO⁺ adduct, which was suggested in the literature [4,5] for similar cases (Scheme 2).



Scheme 3.

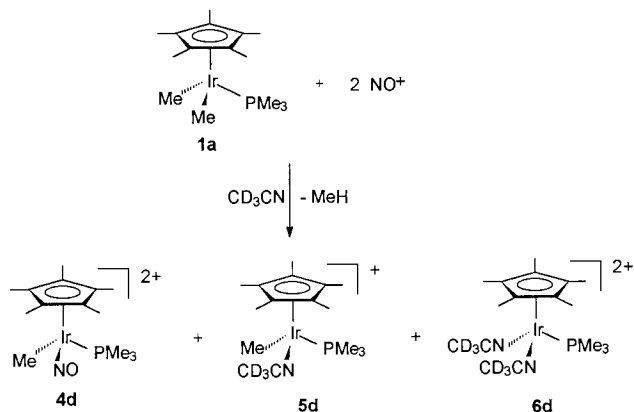
The **1** → **3a** and **1** → **4** reactions should occur through an oxidatively induced cleavage of the Ir–Me bonds resulting in the formation of methane via the C–H activation of the Cp* group with subsequent H abstraction from the solvent, the organometallic fragment being trapped by the phosphine ligand or the nitrosyl cation. Accordingly **3a** was also obtained by treating **1a** with triphenylphosphine in the presence of a classical one-electron oxidant like FeCp₂⁺. Then the formation of **3a** and **4** resembles the reaction of **1a–1d** [2] with pyridine in the presence of an oxidant.

Moreover such reactions seem to mimic the mechanistic steps which are at the basis of the activation of arenes by **1a–1d** under electron transfer catalysis, where, in the absence of better coordinating agents, aryl radicals deriving from the aromatic solvent enter the coordination sphere of the metal [1].

2.2. Reactions of [Ir(Me)₂Cp*(PMe₃)] (**1d**) with NOBF₄ in acetonitrile

Tilset and coworkers [6,7] have studied the oxidation of **1a** and of its rhodium congener in CH₃CN by using Fe(III) complexes. In the case of iridium, methane and the acetonitrile complex [Ir(Me)Cp*(CH₃CN)(PPh₃)]⁺ are the main products [6]. Then it was interesting to study the reaction of the iridium(III) dimethyl derivatives with NOBF₄ in acetonitrile where NO⁺ and CH₃CN could compete in coordinating to the metal centre.

Treatment of **1d** with an equimolar amount of NOBF₄ in CD₃CN produces an immediate variation of colour from light yellow to deep yellow and a vigorous outcome of CH₄ (δ 0.19, singlet) along with the formation of a new organometallic product **5d** (Scheme 3). The ¹H-NMR spectrum of the reaction mixture reveals that the starting substrate was completely consumed after ca. 24 h. The ¹H-NMR spectrum of **5d** displays the presence of one iridium bonded methyl group (doublet at δ 0.44, *J* = 6.6 Hz) in addition to the signal of the Cp* protons (doublet, δ 1.73, *J* = 2.1 Hz) and to the PMe₃ resonances (δ 1.49, *J* = 10.7 Hz). On this basis the compound was formulated as the tetrafluoroborate salt of [Ir(Me)Cp*(CD₃CN)(PMe₃)]⁺, which was also prepared by an alternative route by reaction of [Ir(Me)(Cl)Cp*(PMe₃)] with AgBF₄ in CD₃CN.



Then the reaction is substantially analogous to the oxidation of **1a** with ferrocenium in acetonitrile described in the literature [7].

Treatment of **1d** with an excess of NOBF_4 ($\text{NO}^+/\text{Ir} = 2$) in CD_3CN , causes the colour to change from yellow to deep maroon. The $^1\text{H-NMR}$ spectrum soon after the mixing of the reagents shows that, in addition to CH_4 and **5d**, $[\text{Ir}(\text{Me})\text{Cp}^*(\text{NO})(\text{PMe}_3)](\text{BF}_4)_2$ (**4d**) and $[\text{IrCp}^*(\text{CD}_3\text{CN})_2(\text{PMe}_3)](\text{BF}_4)_2$ (**6d**) are formed (Scheme 4). Complex **6d** was identified by its $^1\text{H-NMR}$ spectrum showing a doublet due to the Cp^* protons (δ 1.79, $J = 2.3$ Hz) and a doublet due to PMe_3 (δ 1.74, $J = 11.8$ Hz), in fair agreement with the data reported in the literature for the triflate salt of the same cation [8]. Finally **6d** was independently prepared by reaction of $[\text{Ir}(\text{Cl})_2\text{Cp}^*(\text{PMe}_3)]$ with an excess of AgBF_4 in CD_3CN .

Complexes **4d**, **5d** and **6d** are initially produced in almost equal amounts, but during the reaction **4d** slowly decreases in favour of **5d** and **6d**; after 7 days

only **5d** and **6d** are present (in a 1/1 ratio). These data suggest that **5d** and **6d** are formed from **4d** by reaction with acetonitrile (since formation of ethane was not observed it is quite improbable that **6d** is a primary oxidation product [6,7]).

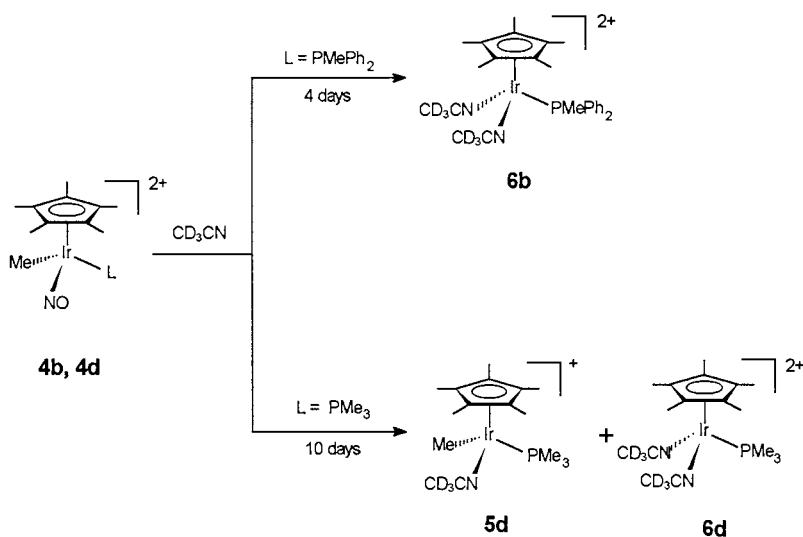
In order to verify this hypothesis we have studied the reactions of isolated **4d** with acetonitrile.

$^1\text{H-NMR}$ spectroscopy shows the slow (10 days) and complete conversion of **4d** into a mixture of **5d** and **6d**, the latter being the major product (1:5) (Scheme 5).

The formation of **5d** and **6d** is interesting since substitution reactions of the nitrosyl ligand are not frequently observed [9]. For instance when both the nitrosyl and carbonyl ligands are present, CO rather than NO is substituted: this is consistent with a stronger M-NO bond compared to the M-CO bond because of the greater backbonding degree of NO [10]. Moreover, as far as we know, cases where the nitrosyl ligand comes out as NO^+ are unknown, and the reason of the unusual behaviour of **4d** is to be attributed to the particularly low Ir-NO bond energy (as inferred from the extremely high value of the NO stretching) being part of a doubly charged complex cation.

The reaction of **4b** with CD_3CN gives quantitatively after 4 days $[\text{IrCp}^*(\text{CD}_3\text{CN})_2(\text{PMePh}_2)]^{2+}$ (**6b**), as shown by the formation in the NMR spectrum of two new doublets due to Cp^* (δ 1.61, $J = 2.2$ Hz) and to PMePh_2 (δ 2.45, $J = 10.7$ Hz). Identification of **6b** was definitely accomplished by comparison of its $^1\text{H-NMR}$ data with those of an authentic sample obtained by reaction of $[\text{IrCl}_2\text{Cp}^*(\text{PMePh}_2)]$ with an excess of AgBF_4 in CD_3CN . In contrast with **4d** no replacement of NO^+ by acetonitrile occurs.

The reactions of both **4b** and **4d** with acetonitrile to give **6b** and **6d** imply the loss of Me and NO from the coordination sphere. Although we have not been able



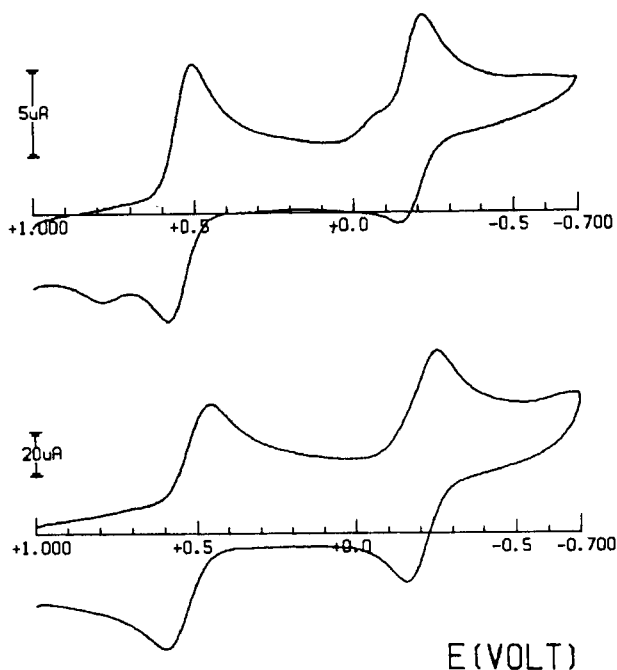


Fig. 4. Cyclic voltammograms recorded at a platinum electrode in solution of **4d** (1.1×10^{-3} mol dm $^{-3}$) in acetone and [NBu $_4$][ClO $_4$] (0.2 mol dm $^{-3}$). Scan rates: (top) 0.1 V s $^{-1}$; (bottom) 5.12 V s $^{-1}$.

to establish the fate of these ligands, a plausible hypothesis is the formation of MeNO, which could eventually dimerize or isomerize [11].

Then the facts concerning the reaction of **1d** with NO $^+$ in acetonitrile may be summarized as following: when equimolar amounts are used, NO $^+$ behaves as a one-electron oxidant and the acetonitrile complex [Ir(Me)Cp*(MeCN)(PMe $_3$)] $^+$ (**5d**) forms, as in the case of the Tilset paper [6]; when two equivalents of NO $^+$ are used, the excess of NO $^+$ acts as the preferred ligand to give **4d**, which slowly undergoes formal substitution of NO $^+$ or MeNO by the acetonitrile solvent to afford **5d** and **6d** respectively.

2.3. Reduction of nitrosyl iridium(III) derivatives [Ir(Me)Cp*(NO)(L)](BF $_4$) $_2$ (L = PMePh $_2$ **4b**, PMe $_2$ Ph **4c**, PMe $_3$ **4d**)

2.3.1. Electrochemical reduction

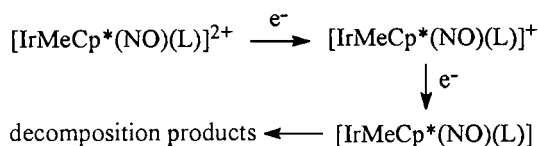
As a typical example of the electrochemical behaviour of the present nitrosyl complexes, Fig. 4 shows the cyclic voltammetric response exhibited by **4d** in acetone solution.

Two subsequent reduction processes appear, the first of which has features of chemical reversibility, whereas the second one is complicated by slow chemical reactions. Only at high scan rates no spurious peaks associated to the second cathodic step are present.

Analysis [12] of the cyclic voltammograms relative to the first reduction with scan rates varying from 0.02 to

1.00 V s $^{-1}$ shows that: (i) the current function $i_{pc}/v^{1/2}$ remains substantially constant; (ii) the current ratio i_{pa}/i_{pc} is constantly equal to 1; (iii) the peak-to-peak separation progressively increases from 65 to 98 mV. These data are representative of a chemically and essentially electrochemically reversible one-electron process. Since the formal electrode reduction of the couple NO $^+$ /NO occurs at quite higher potential values (E° ca. +1.4 V) [13] and in spite of the hard-to-assign nature of redox processes exhibited by metal-NO complexes (see for instance [14]), we preliminarily attribute the reduction process to the iridium(III)/(II) couple, demanding the exact nature of the reduction to the below discussed EPR responses.

Controlled potential coulometry in correspondence to the first reduction step ($E_w = +0.2$ V) consumes one electron/molecule. In confirmation of the chemical reversibility of the first cathodic step, the solution resulting from exhaustive one-electron reduction exhibits a cyclic voltammetric profile quite complementary to the original one. By contrast, the further one-electron reduction at the second cathodic step ($E_w = -0.4$ V) affords a solution which no more exhibits peak-systems related to the original ones.



The formal electrode potentials of the iridium(III)/(II)/(I) redox changes exhibited by the present complexes are compiled in Table 2. The Ir(III)/Ir(II) redox potentials of these complexes follow the electronic effects expected on the basis of the content of methyl groups in the phosphine ligand. This is consistent with the increasing phosphine basicity (pK_a : 4.57 PMePh $_2$; 6.50 PMe $_2$ Ph; 8.65 PMe $_3$) [15], which makes the iridium system having the aliphatic phosphine less prone to reduction.

In all cases the corresponding iridium(II) complexes are relatively stable. In comparison the related rhenium(I) complex [Re(Me)Cp(NO)(PPh $_3$)] undergoes a one-electron oxidation process to the corresponding rhenium(II) congener, which is complicated by chemical reactions [16].

It is also interesting to compare the redox behaviour of the iridium(III) nitrosyl complexes with those of the corresponding complexes **1b**, **1c** and **1d**, in which the nitrosyl group is replaced by a methyl group. As a proof of the strong electronic effects played by the nitrosyl group, **1b**, **1c** and **1d** only undergo one electron oxidation to the corresponding iridium(IV) congeners [1].

Because of the chemical stability of the one-electron reduced complexes, EPR measurements on their ex-

Table 2
Formal electrode potentials (V vs. SCE) and peak-to-peak separations (mV) for the redox changes exhibited by the present iridium(III) alkyl complexes

Complex	$E_{\text{Ir}}^{\text{IV/III}}$	ΔE_p	$E_{\text{Ir}}^{\text{III/II}}$	ΔE_p^a	$E_{\text{Ir}}^{\text{II/I}}$	ΔE_p^a	Solvent
4b			+0.62	90	-0.17	80	Me ₂ CO
4c			+0.59	81	-0.08	90	Me ₂ CO
4d			+0.55	80	-0.22	80	Me ₂ CO
1b	+0.36	80 ^a					CH ₂ Cl ₂
1c	+0.30	120 ^b					CH ₂ Cl ₂
1d	+0.28	114 ^b					CH ₂ Cl ₂

^a Measured at 0.2 V s⁻¹.

^b Measured at 1 V s⁻¹ see Ref. [1c].

haustive one-electron reduced solutions have been performed in order to ascertain the metallic character of the relevant cathodic steps.

Table 3 reports the temperature dependent X-band EPR parameters relevant to the species **7b–7d** obtained by electrochemical reduction of **4b–4d**. The EPR parameters are obtained by computer simulation of the experimental temperature dependent spectra [17]. It is to be noted that all the $S = 1/2$ paramagnetic monocations display completely reversible magnetic behaviour in the experimental temperature range ($T = 100–285$ K). Fig. 5 shows the X-band EPR spectra of the monocation electrogenerated from **4c**, the upper one being recorded at 100 K, the lower one at room temperature. The glassy lineshape is characteristic of a metal-in-character rhombic structure displaying minor spectral resolution in the low-field region; the room-temperature spectrum is unresolved, due to actual $\Delta H_{\text{iso}} >$ of the relevant metal A_{iso} hyperfine splittings (< 40 G).

By comparison of the actual experimental data of the monocations obtained from **4b–4d** with those relevant to the analogous compounds obtained by chemical synthesis (Table 4), it is evident the good agreement between the corresponding paramagnetic parameters, even in the presence of some differences, particularly evident in the case of the species which has been electrogenerated from **4d**. This behaviour is not surprising [1] by considering the different synthesis pathways and, in particular, the non-innocent nature of the sol-

vent in the electrochemical route (acetone), which can act as a better coordinating agent than CH₂Cl₂.

2.3.2. Chemical reduction

The values of the potentials reported in Table 2 indicate that the relatively stable one-electron reduction

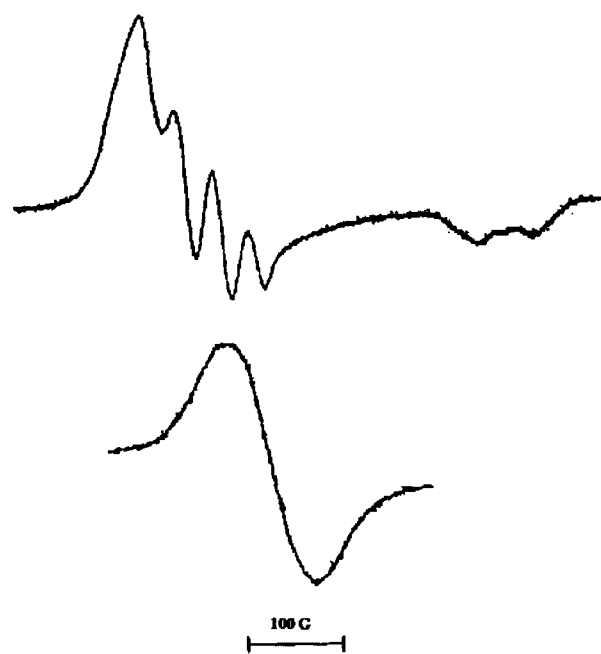


Fig. 5. X-band EPR spectra of the electrogenerated **7c** species. (Top) Liquid nitrogen temperature; (bottom) room temperature.

Table 3
Temperature-dependent X-band EPR parameters of the electrogenerated species **7b–7d**^a

Species	$g_1^{b,c}$	g_2^b	g_3^b	$\langle g \rangle^b$	A_1 (G) ^b	A_2 (G) ^b	A_3 (G) ^b	$\langle A \rangle$ (G) ^b	g_{iso}^d
7b	2.020	1.979	1.810	1.936	16.9	35.3	18.0	24.0	1.929
7c	2.016	1.980	1.807	1.935	20.1	35.0	25.8	26.0	1.932
7d	2.012	1.978	1.813	1.934	21.0	34.5	24.1	25.2	1.927

^a $\langle g \rangle = 1/3(g_1 + g_2 + g_3)$; $\langle A \rangle = 1/3(A_1 + A_2 + A_3)$; $g_i = \pm 0.010$, $A_i = \pm 2$ G; experimental frequency $\nu = 9.44$ GHz.

^b $T = 100$ K.

^c Evaluated by comparison of the relevant room-temperature and frozen solution data.

^d Room temperature.

Table 4
EPR parameters for **7b–7d**

Species	g_1	g_2	g_3	A_1 (G)	A_2 (G)	A_3 (G)
7b	2.009	1.975	1.819	18.40	34.50	16.41
7c	2.014	1.978	1.814	15.82	33.70	25.65
7d	1.949	1.916	1.762	16.77	33.64	25.32

products of **4b–4d** are less easily reduced than **1b⁺–1d⁺**.

Reduction of **4b–4d** with $[\text{CoCp}_2]$ in CH_2Cl_2 has been followed by EPR spectroscopy at temperatures between 93 and 293 K, the signals of the products becoming strong enough to be observed at 223 K. Such signals disappear in a few days at room temperature, because the one-electron reduction products **7b–7d** are further reduced to diamagnetic EPR silent species. This occurs even by using lower than stoichiometric amounts of cobaltocene ($\text{Co}/\text{Ir} = 0.5$) which, being very soluble in CH_2Cl_2 , is still in excess over the almost insoluble dication. **7b–7d** give single line spectra in solution at ca. 193 K, and give well solved EPR spectra showing an hyperfine structure in the glass state at 93 K (Fig. 6).

These spectra consist of three components with some delocalization of the unpaired electron on the iridium nucleus. Then these compounds can be described as low spin iridium(II) complexes having rhombic symmetry. The spectral parameters are obtained by simulation and are reported in Table 4.

Complexes **7b–7d** have been identified as the one-electron reduction products of **4b–4d** with negligible rearrangement of the ligands: actually the EPR parameters are practically identical to those of the electrochemically generated reduction products of **4a–4d**, and electrochemistry has proved the chemical reversibility of the first reduction process. Finally EPR spectra of the isolated **7c** and **7d** (vide infra) are also identical to those reported in Fig. 6.

Reduction of dications **4b–4d** to the corresponding monocations **7b–7d** on a preparative scale has been carried out by slow addition of a benzene solution of cobaltocene to a benzene suspension of the dication. Complex **7b** was too unstable to be isolated, while **7c** and **7d** were isolated as light maroon solids, which are unstable in the air and soluble in dichloromethane, acetone and acetonitrile, and were identified on the basis of the spectroscopic and analytical data (Scheme 6).

IR spectra of **7c** and **7d** in dichloromethane solution show intense N–O stretching absorptions at 1825 and 1823 cm^{-1} , respectively, suggesting a linear coordination for the nitrosyl ligand. These absorptions occur at frequencies which are lower than those of the corresponding dications **4c** (1902 cm^{-1}) and **4d** (1903 cm^{-1}), as expected because of stronger $\text{M} \rightarrow \text{NO}$ back-bonding.

‘Ion-spray’ mass spectrometry in acetonitrile confirms the above assignment. The spectrum of **7c** shows, in addition to the signal at 509/511 (^{191}Ir 59.49, ^{193}Ir 100) corresponding to $[\text{Ir}(\text{Me})\text{Cp}^*(\text{NO})(\text{PMe}_2\text{Ph})]^+$, a peak at m/z 520/522, corresponding to the substitution product of NO by acetonitrile, and peaks at m/z 479/

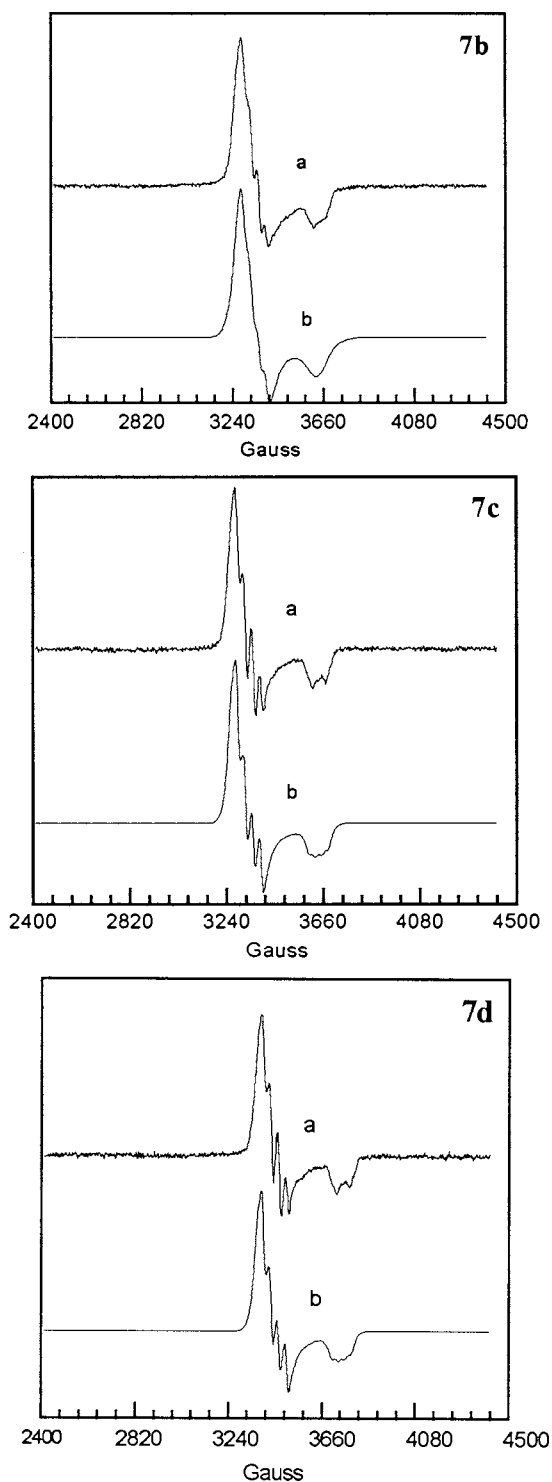
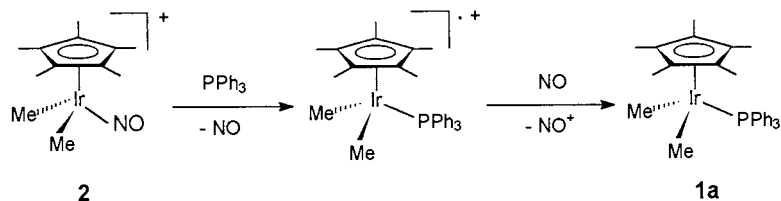


Fig. 6. EPR spectrum of **7c** from the one-electron reduction of **3c** with $[\text{CoCp}_2]$ in CH_2Cl_2 at 93 K; (a) observed; (b) simulated.



Scheme 10.

3. Conclusions

We would like to make a few points on the chemistry of the above cationic iridium nitrosyl derivatives. First of all we would like to comment substitution reactions. As we have described, some of the products of the reaction with acetonitrile or phosphine derive formally from the substitution of NO^+ from the incoming ligand. Of course a possible explanation is that NO is evolved leaving a paramagnetic complex which undergoes a back reaction (Scheme 10), as it has been suggested in the literature [18] for analogous reactions of cationic ruthenium nitrosyl derivatives. In Scheme 10 is reported such a postulated mechanism for the reaction of **2** with PPh_3 . Alternatively one could think of a true displacement of NO^+ from the dicationic complex. More studies are clearly needed in order to fully explain the observed behaviour.

Finally a comment on the EPR spectra of the one-electron reduction products of **4b–4d**, i.e. **7b–7d**. As we have already discussed, such nitrosyl complexes give well solved patterns showing an hyperfine structure and consisting of three components with some delocalization of the unpaired electron on the iridium centre, which can be then described as a low spin iridium(II) system. Now, generally speaking, EPR studies reported in the literature on nitrosyl complexes show invariably the interaction of the unpaired electron with the NO ligand. In such cases the coordination shell of the metal retains its 18e structure, and the radical center is borne by the ligand, and not by the metal. The iridium complexes **7b–7d** show instead a different delocalization of the unpaired electron, as it results from the lack of any hyperfine interaction with the nitrogen, and from the observed coupling to the metal. As far as we know, there are no other cases of a paramagnetic transition metal system carrying a NO group and yet showing no interaction with the nitrogen nucleus [19]. If one can define 19e complexes as having 19 VE with a predominant metal character, this should be the case.

4. Experimental

The reactions and manipulation of organometallics were carried out under dinitrogen or argon, using stan-

dard techniques. The solvents were dried and distilled prior to use. The compounds $[\text{Ir}(\text{Me})_2\text{Cp}^*(\text{L})]$ ($\text{L} = \text{PPh}_3$ (**1a**) [15], PMePh_2 (**1b**) [1c], PMe_2Ph (**1c**) [1c], PMe_3 (**1d**) [1b]), $[\text{Ir}(\text{CD}_3)_2\text{Cp}^*(\text{PMe}_3)]$ [1b], $[\text{Ir}(\text{Me})(\text{Cl})\text{Cp}^*(\text{L})]$ ($\text{L} = \text{PPh}_3$ [20], PMePh_2 [20], PMe_2Ph [1c], PMe_3 [21]) and $[\text{Rh}(\text{Me})_2\text{Cp}^*(\text{PMe}_3)]$ [1b] were prepared according to literature procedures. AgBF_4 and $[\text{FeCp}_2]\text{PF}_6$ were Aldrich products. NOBF_4 (Aldrich product) was treated under vacuum before use. ^1H -, ^{31}P -, ^2H -NMR spectra were recorded on Varian Gemini 200 and VXR 300 instruments. EPR spectra for the chemical oxidation and reduction reactions were obtained by using EPR Varian E 112 instrument equipped with a Varian E 257 for temperature control. The spectrometer was interfaced to an AST Premium 486/25 by means of a data acquisition system consisting of an acquisition board capable of acquiring up to 500 000 12-bit samples s^{-1} , including 32-bit addition to memory, thus giving on-line signal averaging and a software package specially designed for EPR experiments [22]. Materials and apparatus used for electrochemistry and coupled EPR measurements have been described elsewhere [23]. All the potentials values are referred to the saturated calomel electrode (SCE); under the present experimental conditions the one electron oxidation of ferrocene occurs at +0.44 V in dichloromethane solution and at +0.46 V in acetone solution. Elemental analyses were performed by the Laboratorio di Microanalisi of the Istituto di Chimica Organica, Facoltà di Farmacia, University of Pisa.

4.1. EPR spectral studies of the reaction of **1a–1d** with NOBF_4

The reaction mixtures were prepared by placing a weighed amount of metal complex (typically, 5 mg) and NOBF_4 (1–2 mg) into a quartz tube (o.d. 3 mm; i.d. 2 mm) fitted with a quartz–Pyrex joint and a Corning Rotaflo Teflon tap (DISA, Milan). The tube was then attached to a vacuum line and degassed by standard vacuum/argon techniques; afterwards, it was immersed in a dry ice-cooled acetone bath and then charged with dichloromethane under pure argon atmosphere. The quartz tube was then introduced into the spectrometer cavity, pre-cooled to the desired temperature, and then the reagents allowed to mix gradually. The hyperfine

coupling constants and linewidths were obtained by computer simulation of the EPR spectra.

4.2. Reaction of **1a** with NOBF_4 : formation of $[\text{Ir}(\text{Me})_2\text{Cp}^*(\text{NO})]\text{BF}_4$ (**2**) and $[\text{Ir}(\text{Me})\text{Cp}^*(\text{PPh}_3)_2]\text{BF}_4$ (**3a**)

Complex **1a** (0.05 g, 0.081 mmol) was dissolved in CH_2Cl_2 (5 ml) and added with NOBF_4 (0.010 g, 0.081 mmol). Methane (δ 0.20, CD_2Cl_2) evolved and the colour changed from light-yellow to golden-yellow. After stirring for 3 h, the solvent was evaporated to dryness; the residue was washed repeatedly with benzene and dried under vacuum to give a mixture (0.029 g) of **2** (64%) and **3a** (36%). By fractional crystallization from acetone, pure **2** and **3a** were obtained. Complex **2**: Found: C, 30.05; H, 4.40. $\text{C}_{12}\text{H}_{21}\text{BF}_4\text{IrNO}$: Anal. Calc.: C, 30.31; H, 4.45%. IR (Nujol, cm^{-1}) 1843 (s, NO), 1054 (s, BF). $^1\text{H-NMR}$ (CD_3COCD_3): δ 1.81 (6 H, s, IrMe), 2.25 (15 H, s, C_5Me_5). $^1\text{H-NMR}$ (CD_2Cl_2): δ 1.71 (6 H, s, IrMe), 2.14 (15 H, s, C_5Me_5). IS-MS (MeOH), m/e : 386 $[\text{M}]^+$, 370 $[\text{M}-\text{MeH}]^+$, 340 $[\text{M}-\text{MeH}-\text{NO}]^+$, 326 $[\text{IrC}_5\text{Me}_5]^+$, 87 $[\text{BF}_4]^-$. Complex **3a**: Found: C, 58.91; H, 4.91. $\text{C}_{47}\text{H}_{48}\text{BF}_4\text{IrP}_2$: Anal. Calc.: C, 59.10; H, 5.07%. IR (Nujol, cm^{-1}) 1062 (BF_4). $^1\text{H-NMR}$ (CD_3COCD_3): δ 1.26 (15 H, t, $J_{\text{HP}} = 2.2$ Hz, C_5Me_5), 1.56 (3 H, t, $J_{\text{HP}} = 4.9$ Hz, IrMe). $^1\text{H-NMR}$ (CD_2Cl_2): δ 1.19 (15 H, t, C_5Me_5), 1.50 (3 H, t, IrMe); IS-MS (MeOH), m/e : 866 $[\text{M}]^+$, 603 $[\text{M}-\text{PPh}_3]^+$, 587 $[\text{M}-\text{PPh}_3-\text{CH}_4]^+$. The same procedure as above was used when **1a** was reacted with an excess of NOBF_4 .

4.3. Reaction of **1b** with an excess of NOBF_4 in CH_2Cl_2 : formation of $[\text{Ir}(\text{Me})\text{Cp}^*(\text{NO})(\text{PMePh}_2)](\text{BF}_4)_2$ (**4b**)

Complex **1b** (0.1 g, 0.18 mmol) in CH_2Cl_2 (5 ml) was reacted with NOBF_4 (0.042 g, 0.36 mmol). The reaction mixture was stirred at room temperature for 3 h. Methane was evolved and a deep-orange solid was formed, which was washed repeatedly with CH_2Cl_2 and C_6H_6 , and then dried under vacuum. Complex **4b** was obtained as a maroon hygroscopic solid (0.071 g, 53%). Found: C, 36.98; H, 1.71; N, 3.83. $\text{C}_{24}\text{H}_{31}\text{B}_2\text{F}_8\text{IrNOP}$: Anal. Calc.: C, 38.54; H, 1.87; N, 4.18%. IR (Nujol, cm^{-1}) 1900 (s, NO), 1059 (BF_4). $^1\text{H-NMR}$ (CD_3COCD_3): δ 2.25 (3 H, d, $J_{\text{HP}} = 4.8$ Hz, IrMe), 2.30 (15 H, d, $J_{\text{HP}} = 1.9$ Hz, C_5Me_5), 2.96 (3H, d, $J_{\text{HP}} = 11.6$ Hz, PMe), 7.7–8.2 (10 H, bm, Ph). $^1\text{H-NMR}$ (CD_3CN): δ 2.02 (3 H, d, IrMe), 2.09 (15 H, d, C_5Me_5), 2.55 (3H, d, PMe), 7.3–7.65 (10 H, bm, Ph). IS-MS, m/e : 585 $[\text{M}-\text{NO}^+ + \text{MeCN}]^+$, 543 $[\text{M}-\text{NO}^+]^+$, 527 $[\text{M}-\text{NO}^+ \text{MeH}]^+$, 286 $[\text{M}]^{++}$, 263 $[\text{M}-\text{MeNO}]^{++}$, 87 $[\text{BF}_4]^-$.

4.4. Reaction of **1c** with an excess of NOBF_4 in CH_2Cl_2 : formation of $[\text{Ir}(\text{Me})\text{Cp}^*(\text{NO})(\text{PMe}_2\text{Ph})](\text{BF}_4)_2$ (**4c**)

Complex **4c** was prepared as above in 56% yield as a maroon hygroscopic solid. Found: C, 32.87; H, 4.56; N, 1.18. $\text{C}_{19}\text{H}_{29}\text{B}_2\text{F}_8\text{IrNOP}$: Anal. Calc.: C, 33.28; H, 4.27; N, 2.04%. IR (Nujol, cm^{-1}) 1899 (s, NO), 1057 (BF_4). $^1\text{H-NMR}$ (CD_3COCD_3): δ 2.28 (15 H, d, $J_{\text{HP}} = 2.1$ Hz, C_5Me_5), 2.36 (3 H, d, $J_{\text{HP}} = 5.3$ Hz, IrMe), 2.56 (3H, d, $J_{\text{HP}} = 12.5$ Hz, PMe), 2.54 (3 H, d, $J_{\text{HP}} = 11.9$ Hz, PMe). IS-MS (MeCN), m/e : 520 $[\text{M}-\text{NO}^+ + \text{MeCN}]^+$, 479 $[\text{M}-\text{NO}^+]^+$, 463 $[\text{M}-\text{NO}^+ - \text{MeH}]^+$, 273 $[\text{M}-\text{MeNO} + 2\text{MeCN}]^{++}$, 254.7 $[\text{M}]^{++}$, 87 $[\text{BF}_4]^-$.

4.5. Reaction of **1d** with an excess of NOBF_4 in CH_2Cl_2 : formation of $[\text{Ir}(\text{Me})\text{Cp}^*(\text{NO})(\text{PMe}_3)](\text{BF}_4)_2$ (**4d**)

Complex **4d** was prepared as above in 60% yield as a deep orange solid. Found: C, 26.63; H, 4.50; N, 2.21. $\text{C}_{14}\text{H}_{27}\text{B}_2\text{F}_8\text{IrNOP}$: Anal. Calc.: C, 26.96; H, 4.37; N, 2.25%. IR (Nujol, cm^{-1}) 1903 (s, NO), 1056 (s, BF_4). $^1\text{H-NMR}$ (CD_3COCD_3): δ 2.28 (9 H, d, $J_{\text{HP}} = 12.6$ Hz, PMe), 2.31 (3 H, d, $J_{\text{HP}} = 6.2$ Hz, IrMe), 2.53 (15 H, d, $J_{\text{HP}} = 1.9$ Hz, C_5Me_5). $^1\text{H-NMR}$ (CD_3CN): δ 1.97 (9 H, d, PMe), 2.05 (3 H, d, IrMe), 2.28 (15 H, d, C_5Me_5). IS-MS (MeCN), m/e : 460 $[\text{M}-\text{NO}^+ + \text{MeCN}]^+$, 446 $[\text{M}-\text{H}^+]^+$, 417 $[\text{M}-\text{NO}^+]^+$, 401 $[\text{M}-\text{NO}^+ \text{MeH}]^+$, 224 $[\text{M}]^{++}$, 87 $[\text{BF}_4]^-$.

4.6. Reaction of **1d** with equimolar amounts of NOBF_4 in CD_3CN : formation of $[\text{Ir}(\text{Me})\text{Cp}^*(\text{CD}_3\text{CN})(\text{PMe}_3)](\text{BF}_4)$ (**5d**)

Complex **1d** (0.020 g, 0.046 mmol) was dissolved in an NMR tube containing 1 ml of CD_3CN , and NOBF_4 (0.005 g, 0.046 mmol) was added causing an immediate colour variation from light yellow to deep yellow, and gas (CH_4 , δ 0.19) formation. The mixture was stirred at room temperature for 24 h, thereafter the $^1\text{H-NMR}$ spectrum showed the formation of **5d** as the only product. $^1\text{H-NMR}$ (CD_3CN): δ 0.44 (3 H, d, $J_{\text{HP}} = 6.6$ Hz), 1.49 (9 H, d, $J_{\text{HP}} = 10.7$ Hz), 1.73 (15 H, d, $J_{\text{HP}} = 2.1$ Hz).

4.7. Reaction of $[\text{Ir}(\text{Me})(\text{Cl})\text{Cp}^*(\text{PMe}_3)]$ with AgBF_4 in CD_3CN : formation of $[\text{Ir}(\text{Me})\text{Cp}^*(\text{CD}_3\text{CN})(\text{PMe}_3)](\text{BF}_4)_2$ (**6d**)

AgBF_4 (0.011 g, 0.055 mmol) was added to a $^1\text{H-NMR}$ tube containing $[\text{Ir}(\text{Me})(\text{Cl})\text{Cp}^*(\text{PMe}_3)]$ (0.025 g, 0.055 mmol) dissolved in CD_3CN (1 ml). AgCl formed immediately. After 2 h the suspension was filtered and the clear solution examined by $^1\text{H-NMR}$ was found to contain **5d** as the only product.

4.8. Reaction of **1d** with an excess of NOBF_4 in $\text{CD}_3\text{-CN}$: formation of $[\text{Ir}(\text{Me})\text{Cp}^*(\text{NO})(\text{PMe}_3)](\text{BF}_4)_2$ (**4d**), $[\text{Ir}(\text{Me})\text{Cp}^*(\text{CD}_3\text{CN})(\text{PMe}_3)](\text{BF}_4)$ (**5d**) and $[\text{IrCp}^*(\text{CD}_3\text{CN})_2(\text{PMe}_3)](\text{BF}_4)_2$ (**6d**)

Complex **1d** (0.018 g, 0.041 mmol) was dissolved in an NMR tube containing 1 ml of CD_3CN , and NOBF_4 (0.010 g, 0.086 mmol) was added causing an immediate colour variation from light yellow to deep yellow, and gas (CH_4 , δ 0.19) formation. The $^1\text{H-NMR}$ spectrum shows the presence of **4d**, **5d** and **6d** in roughly equivalent amounts. After 1 week at room temperature, only **5d** and **6d** are present in equimolar ratio (by $^1\text{H-NMR}$). Complex **6d**: $^1\text{H-NMR}$ (CD_3CN): δ 1.74 (9 H, d, $J_{\text{HP}} = 11.8$ Hz), 1.79 (15 H, d, $J_{\text{HP}} = 2.3$ Hz).

4.9. Reaction of $[\text{IrCl}_2\text{Cp}^*(\text{PMe}_3)]$ with AgBF_4 in CD_3CN : formation of $[\text{IrCp}^*(\text{CD}_3\text{CN})_2(\text{PMe}_3)](\text{BF}_4)_2$ (**6d**)

AgBF_4 (0.016 g, 0.084 mmol) was added to a $^1\text{H-NMR}$ tube containing $[\text{IrCl}_2\text{Cp}^*(\text{PMe}_3)]$ (0.02 g, 0.042 mmol) dissolved in CD_3CN (1 ml). AgCl formed immediately. After 2 h the suspension was filtered and the clear solution examined by $^1\text{H-NMR}$ was found to contain **6d** as the only product.

4.10. Reaction of $[\text{Ir}(\text{Me})\text{Cp}^*(\text{NO})(\text{PMePh}_2)](\text{BF}_4)_2$ (**4b**) with CD_3CN : formation of $[\text{IrCp}^*(\text{CD}_3\text{CN})_2(\text{PMePh}_2)](\text{BF}_4)_2$ (**6b**)

A sample of $[\text{Ir}(\text{Me})\text{Cp}^*(\text{NO})(\text{PMePh}_2)](\text{BF}_4)_2$ (**4b**) (0.030 g, 0.040 mmol) was dissolved in an NMR tube containing 1 ml of CD_3CN . The $^1\text{H-NMR}$ spectrum shows the formation of a new compound in addition to the starting product. After 4 days **4b** was quantitatively converted into $[\text{IrCp}^*(\text{CD}_3\text{CN})_2(\text{PMePh}_2)](\text{BF}_4)_2$ (**6b**), identified by comparison of the $^1\text{H-NMR}$ spectrum with that of a sample obtained by synthesis. $^1\text{H-NMR}$ (CD_3CN): δ 1.61 (15 H, d, $J_{\text{HP}} = 2.2$ Hz, C_5Me_5), 2.45 (3 H, d, $J_{\text{HP}} = 10.7$ Hz, PMe). $^{31}\text{P-NMR}$ (CD_3CN): δ -3.62.

4.11. EPR spectral studies of the reaction of **4b–4d** with $[\text{CoCp}_2]$

By using the same procedure described in 4.1, **4b–4d** (typically ca. 5 mg) were reacted with CoCp_2 (ca. 2 mg) in CH_2Cl_2 .

4.12. Reaction of $[\text{Ir}(\text{Me})\text{Cp}^*(\text{NO})(\text{PMe}_2\text{Ph})](\text{BF}_4)_2$ (**4c**) with $[\text{CoCp}_2]$: formation of $[\text{Ir}(\text{Me})\text{Cp}^*(\text{NO})(\text{PMe}_2\text{Ph})]\text{-BF}_4$ (**7c**)

A total of 9.5 ml of a benzene solution of cobaltocene (0.024 M, 0.23 mmol) were added dropwise to a

stirred suspension of $[\text{Ir}(\text{Me})\text{Cp}^*(\text{NO})(\text{PMe}_2\text{Ph})](\text{BF}_4)_2$ (**4c**) (0.038 g, 0.055 mmol), in benzene (1 ml). After the addition was over (ca. 1 h) the reaction mixture was stirred for 2 h at room temperature. A solid formed, which was separated from the solution, washed with benzene and dried under vacuum. The solid was extracted with CH_2Cl_2 (5 ml), and the clear solution resulting from the filtration, was dried under vacuum to give a light-maroon residue which was identified as $[\text{Ir}(\text{Me})\text{Cp}^*(\text{NO})(\text{PMe}_2\text{Ph})]\text{BF}_4$ (**7c**) (yield 35%). Found: C, 36.89; H, 4.50; N, 1.85. $\text{C}_{19}\text{H}_{29}\text{BF}_4\text{IrNOP}$: Anal. Calc.: C, 38.12; H, 4.89; N, 2.34%. FT-IR (CH_2Cl_2): 1825 (s, NO); 1078 (s, BF) cm^{-1} . IS-MS (CH_3CN): m/e 520 $[\text{M-NO} + \text{MeCN}]^+$; 509 $[\text{M}]^+$; 479 $[\text{M-NO}]^+$; 463 $[\text{M-NO-CH}_4]^+$.

4.13. Reaction of $[\text{Ir}(\text{Me})\text{Cp}^*(\text{NO})(\text{PMe}_3)](\text{BF}_4)_2$ (**4d**) with $[\text{CoCp}_2]$: formation of $[\text{Ir}(\text{Me})\text{Cp}^*(\text{NO})(\text{PMe}_3)](\text{BF}_4)$ (**7d**)

A total of 9 ml of a benzene solution of cobaltocene (0.024 M, 0.22 mmol) were added dropwise under stirring to a suspension of $[\text{Ir}(\text{Me})(\text{NO})\text{Cp}^*(\text{PMe}_3)](\text{BF}_4)_2$ (**4d**) (0.032 g, 0.052 mmol) in benzene (1 ml). After the addition was over (ca. 1 h), the reaction mixture was stirred for further 2 h. A solid was separated from the solution, washed repeatedly with benzene and dried under vacuum. The resulting dark maroon solid was treated with 5 ml of CH_2Cl_2 , and after filtration the clear solution was dried under vacuum to give $[\text{Ir}(\text{Me})(\text{NO})\text{Cp}^*(\text{PMe}_3)]\text{BF}_4$ (**7d**) as a light maroon solid (45%). Found: C, 30.85; H, 4.64; N, 2.21. $\text{C}_{14}\text{H}_{27}\text{BF}_4\text{IrNOP}$: Anal. Calc.: C, 31.33; H, 5.08; N, 2.61%. FT-IR (CH_2Cl_2): 1823 (s, NO); 1071 (s, BF) cm^{-1} . IS-MS (CH_3CN): m/e 458 $[\text{M-NO} + \text{MeCN}]^+$; 417 $[\text{M-NO}]^+$; 401 $[\text{M-NO-CH}_4]^+$.

4.14. Reaction of $[\text{Ir}(\text{Me})\text{Cp}^*(\text{NO})(\text{PMe}_3)]\text{BF}_4$ (**7d**) with CD_3CN : formation of $[\text{Ir}(\text{Me})\text{Cp}^*(\text{CD}_3\text{CN})\text{-}(\text{PMe}_3)]\text{BF}_4$ (**5d**)

$[\text{Ir}(\text{Me})\text{Cp}^*(\text{NO})(\text{PMe}_3)]\text{BF}_4$ (**7d**) (0.030 g, 0.056 mmol) was dissolved in a NMR tube containing 1 ml of CD_3CN . The $^1\text{H-NMR}$ spectrum showed exclusively the signals of a product which has been identified as $[\text{Ir}(\text{Me})\text{Cp}^*(\text{CD}_3\text{CN})(\text{PMe}_3)]\text{BF}_4$ (**5d**) by comparison with the $^1\text{H-NMR}$ of an authentic sample.

4.15. Reaction of $[\text{Ir}(\text{Me})\text{Cp}^*(\text{NO})(\text{PMe}_3)]\text{BF}_4$ (**7d**) with NOBF_4 : formation of $[\text{Ir}(\text{Me})\text{Cp}^*(\text{NO})(\text{PMe}_3)]\text{-}(\text{BF}_4)_2$ (**4d**)

NOBF_4 (0.023 g, 0.020 mmol) was added to a CH_2Cl_2 solution (3 ml) of $[\text{Ir}(\text{Me})\text{Cp}^*(\text{NO})(\text{PMe}_3)]\text{BF}_4$ (**7d**) (0.011 g, 0.020 mmol). Soon after the mixing of the reactants, a solid deep-maroon formed which, after 1 h

of stirring, was separated from the solution, washed repeatedly with CH_2Cl_2 and dried. The solid resulted to be $[\text{Ir}(\text{Me})\text{Cp}^*(\text{NO})(\text{PMe}_3)](\text{BF}_4)_2$ (**4d**) (60%) identified by comparison with an authentic sample.

4.16. Reaction of $[\text{Ir}(\text{Me})_2\text{Cp}^*(\text{NO})]\text{BF}_4$ (**2**) with PPh_3

A solution of PPh_3 (0.005 g, 0.020 mmol) in 0.7 ml of CD_2Cl_2 was added to $[\text{Ir}(\text{Me})_2\text{Cp}^*(\text{NO})]\text{BF}_4$ (0.020 mmol) (**2**). The colour of the solution changed immediately from yellow to maroon. The $^1\text{H-NMR}$ spectrum showed only the presence of $[\text{Ir}(\text{Me})_2\text{Cp}^*(\text{PPh}_3)]$ (**1a**). $^1\text{H-NMR}$ (CD_2Cl_2): δ -0.05 (6 H, d, $J_{\text{HP}} = 5.0$ Hz, IrMe), 1.39 (15 H, d, $J_{\text{HP}} = 1.8$ Hz, C_5Me_5), 7.15–7.55 (15 H, m, PPh_3).

4.17. Reaction of $[\text{Ir}(\text{Me})\text{Cp}^*(\text{NO})(\text{PMePh}_2)](\text{BF}_4)_2$ (**4b**) with PMePh_2 : formation of $[\text{Ir}(\text{Me})\text{Cp}^*(\text{PMePh}_2)_2]\text{BF}_4$ (**3b**)

PMe_2Ph (0.011 ml, 0.080 mmol) was added to $[\text{Ir}(\text{Me})\text{Cp}^*(\text{NO})(\text{PMe}_2\text{Ph})](\text{BF}_4)_2$ (**4b**) (0.020 g, 0.027 mmol) in acetone (3 ml). The reaction mixture was stirred for 1 h, then evaporation of the solvent under reduced pressure gave a maroon oil, identified as $[\text{Ir}(\text{Me})\text{Cp}^*(\text{PMePh}_2)_2]\text{BF}_4$ (**3b**) (98% yield) by comparison of the $^1\text{H-NMR}$ spectrum with that of a sample prepared as described in Section 4.19.

4.18. Reaction of $[\text{Ir}(\text{Me})\text{Cp}^*(\text{NO})(\text{PMe}_2\text{Ph})](\text{BF}_4)_2$ (**4c**) with PMe_2Ph : formation of $[\text{Ir}(\text{Me})\text{Cp}^*(\text{PMe}_2\text{Ph})_2]\text{BF}_4$ (**3c**)

A solution of PMe_2Ph (0.0125 ml, 0.0875 mmol) in acetone (3 ml) was added to $[\text{Ir}(\text{Me})\text{Cp}^*(\text{NO})(\text{PMe}_2\text{-Ph})](\text{BF}_4)_2$ (**4c**) (0.020 g, 0.029 mmol). The colour changed from deep-maroon to pale-yellow. The mixture was stirred for 1 hr. By evaporation at reduced pressure, an oil was obtained and washed repeatedly with ether to give $[\text{Ir}(\text{Me})\text{Cp}^*(\text{PMe}_2\text{Ph})_2]\text{BF}_4$ (**3c**) as a light-maroon solid, identified by comparison with a sample obtained as described in Section 4.19.

4.19. Reaction of $[\text{Ir}(\text{Me})(\text{Cl})\text{Cp}^*(\text{L})]$ ($\text{L} = \text{PPh}_3, \text{PMePh}_2, \text{PMe}_2\text{Ph}$) with AgBF_4 in the presence of L : formation of **3a**, **3b**, **3c** and **3d**

The reaction of $[\text{Ir}(\text{Me})(\text{Cl})\text{Cp}^*(\text{PPh}_3)]$ with AgBF_4 and PPh_3 in CH_2Cl_2 is reported as an example. PPh_3 (0.008 g, 0.031 mmol) and AgBF_4 (0.006 g, 0.031 mmol) were added under stirring to a CH_2Cl_2 solution (1 ml) containing $[\text{Ir}(\text{Me})(\text{Cl})\text{Cp}^*(\text{PPh}_3)]$ (0.020 g, 0.031 mmol). AgCl precipitated immediately, and, after stirring for 2 h, was filtered off. The resulting clear solution was dried under vacuum. The residue was washed

with pentane, and dried under vacuum to give 0.024 g (81%) of $[\text{Ir}(\text{Me})\text{Cp}^*(\text{PPh}_3)_2]\text{BF}_4$ (**3a**).

The complexes **3b–3c** have been prepared in a similar way from $[\text{Ir}(\text{Me})(\text{Cl})\text{Cp}^*(\text{PMePh}_2)]$ and $[\text{Ir}(\text{Me})(\text{Cl})\text{Cp}^*(\text{PMe}_2\text{Ph})]$ by reaction with PMePh_2 and PMe_2Ph , respectively.

Complex **3a**: $^1\text{H-NMR}$ (CD_2Cl_2): δ 1.19 (15 H, t, $J_{\text{HP}} = 2.2$ Hz, C_5Me_5); 1.50 (3H, t, $J_{\text{HP}} = 4.9$ Hz, IrMe). $^1\text{H-NMR}$ (CD_3COCD_3): δ 1.26 (15H, t, C_5Me_5), 1.56 (3H, t, IrMe). IS-MS (CH_3OH): m/e 866 $[\text{M}]^+$; 603 $[\text{M}-\text{PPh}_3]^+$; 587 $[\text{M}-\text{PPh}_3-\text{CH}_4]^+$.

Complex **3b**: Found: C, 54.20; H, 5.31. $\text{C}_{37}\text{H}_{44}\text{BF}_4\text{IrP}_2$: Anal. Calc.: C, 53.48; H, 5.34%. $^1\text{H-NMR}$ (CD_2Cl_2): δ 1.01 (3 H, t, $J_{\text{HP}} = 5.4$ Hz, IrMe), 1.35 (3 H, d, $J_{\text{HP}} = 10.0$ Hz, PMe), 1.40 (15 H, t, $J_{\text{HP}} = 2.2$ Hz, C_5Me_5), 7.20–7.60 (10 H, bm, Ph).

Complex **3c**: Found: C, 45.33; H, 6.12. $\text{C}_{27}\text{H}_{40}\text{BF}_4\text{IrP}_2$: Anal. Calc.: C, 45.88; H, 5.71%. $^1\text{H-NMR}$ (CD_2Cl_2): δ 0.54 (3 H, t, $J_{\text{HP}} = 6.0$ Hz, IrMe), 1.50 (6 H, d, $J_{\text{HP}} = 10.0$ Hz), 1.58 (15 H, t, $J_{\text{HP}} = 2.0$ Hz, C_5Me_5), 7.2–7.60 (5 H, bm, Ph).

Complex **3d**: $^1\text{H-NMR}$ (CD_3COCD_3): δ 1.88 (15 H, t, $J_{\text{HP}} = 1.9$ Hz, C_5Me_5), 1.66 (18 H, vt, $J_{\text{HP}} = 10.4$ Hz, PMe_3), 0.24 (3H, t, $J_{\text{HP}} = 6.3$ Hz, IrMe).

Acknowledgements

We thank CNR (Rome) for financial support. P.Z. acknowledges the technical assistance of G. Montomoli. P.D. acknowledges the assistance of F. Simoncini and V. Ermini.

References

- [1] (a) P. Diversi, S. Iacononi, G. Ingrosso, F. Laschi, A. Lucherini, P. Zanello, *J. Chem. Soc. Dalton Commun.* (1993) 351. (b) P. Diversi, S. Iacononi, G. Ingrosso, F. Laschi, A. Lucherini, C. Pinzino, G. Uccello-Barretta, P. Zanello, *Organometallics* 14 (1995) 3275. (c) F. de Biani Fabrizi, P. Diversi, A. Ferrarini, G. Ingrosso, F. Laschi, A. Lucherini, C. Pinzino, G. Uccello-Barretta, P. Zanello, *Gazz. Chim. It.* 126 (1996) 391.
- [2] P. Diversi, V. Ermini, G. Ingrosso, A. Lucherini, C. Pinzino, F. Simoncini, *J. Organomet. Chem.* 555 (1998) 135.
- [3] K.J. Mattson, R.B. Clarkson, R.L. Belford, 11th International EPR Symposium, 30th Rocky Mountains Conference, Denver, CO, USA, August 1988.
- [4] N.G. Connelly, W.E. Geiger, *Chem. Rev.* 96 (1996) 877.
- [5] N.G. Connelly, Z. Demidowicz, R.L. Kelly, *J. Chem. Soc. Dalton Trans.* (1975) 2335.
- [6] A. Pedersen, M. Tilset, *Organometallics* 12 (1993) 56.
- [7] A. Pedersen, M. Tilset, *Organometallics* 13 (1994) 4887.
- [8] P.J. Stang, Y.-H. Huang, A.M. Arif, *Organometallics* 11 (1992) 231.
- [9] G.B. Richter-Addo, P. Legzdins, *Chem. Rev.* 88 (1988) 991.
- [10] (a) C.A. Reed, W.R. Roper, *J. Chem. Soc. A* (1970) 3054. (b) M. Kubota, M.K. Chan, *Inorg. Chem.* 23 (1984) 1636.
- [11] D. Barton, D. Ollis, 1983, in: *Comprehensive Organometallic Chemistry*, vol. 2, Pergamon Press, Oxford, UK, Section 7.1.

- [12] E.R. Brown, J.R. Sandifer, in: B.W. Rossiter, J.F. Hamilton (Eds.), *Physical Methods of Chemistry: Electrochemical Methods*, vol. 2, Wiley, New York, 1986.
- [13] K.Y. Lee, D.J. Kuchynka, J.K. Kochi, *Inorg. Chem.* 29 (1990) 4196.
- [14] (a) N.G. Connelly, S.J. Raven, W.E. Geiger, *J. Chem. Soc. Dalton Trans.* (1987) 467. (b) M.R. Rhodes, M.H. Barley, T.J. Meyer, *Inorg. Chem.* 30 (1991) 629. (c) D. Ooyama, Y. Miura, Y. Kanazawa, F.S. Howell, N. Nagao, M. Mukaida, H. Nagao, K. Tanaka, *Inorg. Chim. Acta* 237 (1995) 47.
- [15] M.M. Rahman, H.-Y. Liu, K. Eriks, A. Prock, W.P. Giering, *Organometallics* 8 (1989) 1.
- [16] M.F. Asaro, G.S. Bodner, J.A. Gladysz, S.R. Cooper, N.J. Cooper, *Organometallics* 4 (1985) 1020.
- [17] G.P. Lozos, G.B. Hoffman, C.G. Franz, SIM14a: Simulation of Powder EPR Spectra, QCPE Program No. 265.
- [18] R.W. Callahan, T.J. Meyer, *Inorg. Chem.* 3 (1977) 574.
- [19] D. Astruc, *Chem. Rev.* 88 (1988) 1189.
- [20] D.S. Glueck, R.G. Bergman, *Organometallics* 10 (1991) 1479.
- [21] J.M. Buchanan, J.M. Striker, R.G. Bergman, *J. Am. Chem. Soc.* 108 (1986) 1537.
- [22] R. Ambrosetti, D. Ricci, *Rev. Sci. Instrum.* 62 (1991) 2281.
- [23] D. Osella, M. Ravera, C. Nervi, C.E. Housecroft, P.R. Raithby, P. Zanello, F. Laschi, *Organometallics* 10 (1991) 3253.